"*Ca.* Nitrosocosmicus" members are the dominant archaea associated with pepper (*Capsicum annuum* L.) and ginseng (*Panax ginseng* C.A. Mey.) plants' rhizospheres

Ui-Ju Lee[1,*], Joo-Han Gwak[1,*], Seungyeon Choi[1], Man-Young Jung[2], Tae Kwon Lee[3], Hojin Ryu[1], Samuel Imisi Awala[1], Wolfgang Wanek[4,5], Michael Wagner[5,6,7], Zhe-Xue Quan[8] & Sung-Keun Rhee[1]

[1]Department of Biological Sciences and Biotechnology, Chungbuk National University, 1 Chungdae-ro, Seowon-Gu, Cheongju 28644, Republic of Korea. [2]Department of Science Education, Jeju National University, 102 Jejudaehak-ro, Jeju 63243, Korea. [3]Department of Environmental Engineering, Yonsei University, Wonju, Republic of Korea. [4]Division of Terrestrial Ecosystem Research, Center of Microbiology and Environmental Systems Science, University of Vienna, Djerassiplatz 1, A-1030 Vienna, Austria. [5]Department of Microbiology and Ecosystem Science, Centre for Microbiology and Environmental Systems Science, University of Vienna, Vienna, Austria. [6]The Comammox Research Platform, University of Vienna, Vienna, Austria. [7]Center for Microbial Communities, Department of Chemistry and Bioscience, Aalborg University, Aalborg, Denmark. [8]School of Life Sciences, Fudan University, Shanghai, China.

[*]These authors contributed equally to this work.

Corresponding author: Sung-Keun Rhee

Email: rhees@chungbuk.ac.kr

Abstract

Background: Although archaea are widespread in terrestrial environments, little is known about the selection forces that shape their composition, functions, survival, and proliferation strategies in the rhizosphere. The ammonia-oxidizing archaea (AOA), which are abundant in soil environments, catalyze the first step of nitrification and have the potential to influence plant growth and development significantly.

Results: Based on archaeal 16S rRNA and *amoA* gene (encoding the ammonia monooxygenase subunit A) amplicon sequencing analysis, distinct archaeal communities dominated by AOA were found to be associated with the root systems of pepper (*Capsicum annuum* L.) and ginseng (*Panax ginseng* C.A. Mey.) plants compared to bulk soil not penetrated by roots. AOA related to "*Candidatus* Nitrosocosmicus", which, unlike most other AOA, harbor genes encoding manganese catalase (MnKat), dominated rhizosphere soils, and thus contributed to the development of distinct archaeal communities in rhizospheres. Accordingly, for both plant species, the copy number ratios of AOA MnKat genes to *amoA* genes were significantly higher in rhizosphere soils than in bulk soils. In contrast to MnKat-negative strains from other AOA clades, the catalase activity of a representative isolate of "*Ca.* Nitrosocosmicus" was demonstrated. Members of this clade were enriched in H_2O_2-amended bulk soils, and constitutive expression of their MnKat gene was observed in both bulk and rhizosphere soils.

Conclusions: Due to their abundance, "*Ca.* Nitrosocosmicus" members can be considered key players mediating the nitrification process in rhizospheres. The selection of this MnKat-containing AOA in rhizospheres of several agriculturally important plants hints at a previously overlooked AOA-plant interaction. For additional mechanistic analyses of the interaction, this key clade of AOA with cultured representatives can be employed.

Introduction

Plants are rooted in soil and thus interact with the rhizosphere microbiome, which has been proposed to confer specific functions to their host plant, by modulating plant nutrient uptake, stress resistance, growth, and health [1, 2, 3]. Soil types and characteristics of soil are primarily shown to determine the background (bulk soil) microbiome, from which rhizosphere microbiomes are selected [4, 5, 6, 7, 8, 9]. Due to rhizodeposition, rhizospheres have higher microbial abundances and distinct microbial communities than bulk soil [10, 11, 12, 13]. The phylogeny or genotype of a plant also contributes to the development of distinct microbial communities in the plant rhizosphere [4, 13, 14].

Plant root exudates influence rhizosphere microbial community development by stimulating or inhibiting specific types of microorganisms [9, 15, 16, 17]. Depending on the mode of photosynthesis [18] as well as the physiological and developmental status of the plant [19, 20, 21], roots release different types of exudates into the rhizosphere. It has also been demonstrated that the rhizosphere microbiome affects root exudation inversely [2]. Even further, it has been postulated that plants actively recruit soil microorganisms by releasing specific compounds into their rhizosphere that selectively stimulate specific microorganisms that are beneficial to plant growth and health [22, 23, 24]. Signal molecules and antimicrobial compounds found in root exudates, such as phytoanticipins, phytoalexins, and sorgoleone, can be critical factors for shaping rhizosphere microbial communities [25, 26, 27, 28]. While we have gained a better understanding of the biology of root development as well as the structure and function of microbial communities in the rhizosphere, the interactions between rhizosphere microbiomes and plant roots via exudate secretion are not well understood [29].

Several studies on the rhizosphere microbiome have been conducted over the years.

However, only a few of them have focused on the archaeal microbiome of roots [14, 30, 31, 32, 33]. Although archaea are widespread in terrestrial environments [34, 35, 36, 37], little is known about selection forces that shape their composition as well as their functions, survival, and proliferation strategies in the rhizosphere [38]. *Nitrososphaerota* (formerly known as Thaumarchaeota) are the predominant archaea found in soil [31, 35]. Members of *Nitrososphaerota* belonging to groups I.1a, I.1a-associated, and I.1b [39, 40] are ammonia-oxidizing archaea (AOA) involved in autotrophic ammonia oxidation, a key step in the nitrification process [36]. Nitrification changes the availability of nitrogen species to plants and thus affects nitrogen fertilizer efficiency and enhances nitrogen mobility in the environment, resulting in fertilizer loss and eutrophication of water bodies. Additionally, the nitrification intermediate, NO, functions as a signaling molecule in plants [41], and ammonia-oxidizing microorganisms (AOM) also produce and emitted N_2O from agricultural soil [42].

Here, we analyzed archaeal communities associated with the rhizosphere of pepper and ginseng plants. The majority of the archaea identified in bulk and rhizosphere soils were AOA-related, and they were frequently found to outnumber ammonia-oxidizing bacteria (AOB) in both bulk and rhizosphere soils. Furthermore, AOA communities differed between bulk and rhizosphere soils, with the latter dominated by AOA closely related to "Candidatus Nitrosocosmicus," a known manganese catalase (MnKat)-containing AOA. Reactive oxygen species (ROS) are produced in the rhizosphere via a variety of metabolic pathways, most of which are attributed to lignin polymerization in plant root cell walls [43, 44, 45], oxidative stress responses through superoxide dismutase, and peroxidase activities of plant and microbes [45, 46, 47]. As a result, we propose that H_2O_2 resistance may be a key factor shaping AOA communities in rhizosphere.

Materials and methods

Plant cultivation, soil collection, and analysis

Soil samples from the bulk and rhizosphere of pepper (*Capsicum annuum* L., Solanaceae) and ginseng (*Panax ginseng* C.A. Meyer, Araliaceae) plants were collected to investigate the plant-root-associated prokaryotic communities. The pepper plants were grown in sandy loam soil under a rain shelter for six months (March to September 2017), with the addition of ammonium sulfate (55 kg N ha^{-1}) as a nitrogen fertilizer once before transplanting. After transplanting, the average temperature in the rain shelter was kept at 25 ± 5 °C, and the soil was watered daily as needed to keep soil moisture above 20% at 30 cm soil depth. Bulk and rhizosphere soils were collected at two different growth phases: vegetative growth (60 days) and reproductive growth (90 days). The rhizosphere soil samples were collected as soil tightly adhering to plant roots. Five bulk soil subsamples were collected at 15 cm soil depth and 40 cm away from the plants and then mixed. The soil samples were stored at −80 °C until DNA extraction. The locations and general properties of bulk soil are presented in Table S1.

The ginseng plants were grown for 6 years (2012-2018) after transplanting one-year-old seedlings (Table S1) to a sandy loam soil field. The Ginseng Good Agricultural Practices Scheme from the National Institute of Horticultural and Herbal Science of the Rural Development Administration (Republic of Korea) was followed for pre-planting treatment, pest management, watering, and fertilization. During the cultivation period, bulk and rhizosphere soils of 2-, 4-, and 6-year-old ginseng plants were collected. The collection of soil samples and analysis of general properties of soils were conducted in the same manner as

113 described above for pepper plants.

114

115 **DNA extraction and quantification of AOA *amoA* and MnKat genes**

116 Genomic DNA was extracted from each 0.25 g soil sample using the Exgene™ Soil DNA mini
117 extraction kit (GeneAll Biotechnology Co. Ltd., Republic of Korea) according to the
118 manufacturer's instructions. The DNA concentration and purity were measured using a
119 Nanodrop ND-1000 spectrophotometer (NanoDrop Technologies, USA). To check for possible
120 quantitative PCR (qPCR) or PCR inhibition, genomic DNA from *Methylacidiphilum*
121 *caldifontis* IT6 (10^6 gene copy numbers per reaction) [48] was spiked as an internal positive
122 control [49] into serially diluted template DNA (0.25–20 ng) extracted from soils of the pepper
123 and ginseng plants. Strain IT6-specific *pmoA1* gene primer pair was used for qPCR detection.
124 The quantitative results of the spiked control within the template or pure water were assessed
125 by comparing the Ct values of the *pmoA1* gene. No significant PCR inhibition was observed in
126 the serially diluted template DNA (0.25–20 ng), and thus, we used < 10 ng DNA for further
127 qPCR analysis.

128 The copy numbers of AOA *amoA* gene were assessed using the
129 CrenamoA104F/CrenamoA616R primer pairs (see Table S2). The primer pair for quantifying
130 AOA MnKat gene (aoa-MnKat200F: 5'-GAAGAGATRGGWCATGTWGA-3', aoa-
131 MnKat480R: 5'-CCTGTMGCYTCAAGCATDA-3') was newly designed using MnKat gene
132 sequences retrieved from the genomes of "*Ca*. Nitrosocosmicus oleophilus" MY3
133 (GCA_000802205.2), "*Ca*. Nitrosocosmicus arcticus" Kfb (GCA_007826885.1), "*Ca*.
134 Nitrosocosmicus hydrocola" G61 (GCF_001870125.1), and "*Ca*.

Nitrososphaera everglandensis" SR1 (GCA_000730285.1). 1−10 ng of sample DNA was used for qPCR using a MiniOpticon qPCR detection system (Bio-Rad Laboratories, Hercules, USA). The iQ SYBR Green Supermix (Bio-Rad Laboratories, USA) and PCR primer pairs were used for PCR amplification. AOA *amoA* gene was amplified via the following steps: 95 °C for 3 min; followed by 40 cycles at 95 °C for 45 s, 55 °C for 45 s, 72 °C for 45 s; and 72 °C for 5 min. AOA MnKat gene was amplified via the following steps: 95 °C for 3 min; followed by 40 cycles at 95 °C for 45 s, 55 °C for 45 s, 72 °C for 45 s; and 72 °C for 5 min. A dilution series of genomic DNA from strain MY3 was included in every qPCR cycle for calibration purposes. Amplification efficiencies ranged between 80 and 94% for all target genes, and qPCR R^2 calibration values were greater than 0.99.

Amplicon sequencing and phylogenetic analysis

For the construction of amplicon sequencing libraries, the 16S rRNA gene was amplified using the 515F/926R primer pairs (see Table S3), via the following steps: 95 °C for 3 min; followed by 25 cycles at 95 °C for 45 s, 50 °C for 45 s, 72 °C for 90 s; and 72 °C for 5 min. AOA *amoA* gene was amplified with the CrenamoA104F/CrenamoA616R primer pairs (see Table S2), via the following steps: 95 °C for 3 min; followed by 30 cycles at 95 °C for 45 s, 55 °C for 45 s, 72 °C for 45 s; and 72 °C for 5 min. AOA MnKat gene was amplified with the aoa-MnKat200F/aoa-MnKat480R primer pairs via the following steps: 3 min heating step at 95 °C; followed by 35 cycles at 95 °C for 45 s, 55 °C for 45 s, 72 °C for 45 s; and 72 °C for 5 min. The following index PCR for both gene libraries was conducted with the Nextera XT index kit v2 (Illumina Inc., USA). The PCR product was purified using the Labopass™ DNA purification kit (Cosmogenetech Inc., Republic of Korea). The sequencing was performed

158 using the Illumina MiSeq (2 × 300 bp) platform (Illumina Inc., USA) at Macrogen Inc.
159 (Republic of Korea). The QIIME2 (v2022.2) pipeline with implemented tools for quality
160 control (Cutadapt) [50], de-noising and pair read merging (DADA2) [51], and *de novo* OTU
161 clustering (VSEARCH) [52] was used to analyze the amplicon sequence data. The primer
162 region was trimmed. After quality plots were generated, the sequences failing to pass an
163 average base call accuracy of 99% (median Phred score of 20) were excluded. Low-quality
164 regions of each sequence were removed during the de-noising step using DADA2 with the
165 following parameters: 16S rRNA gene: --p-trunc-len-f 264 --p-trunc-len-r 168 --p-max-ee-f 2
166 --p-max-ee-r 4; AOA *amoA* gene: --p-trunc-len-f 280 --p-trunc-len-r 265 --p-max-ee-f 2 --p-
167 max-ee-r 4; AOA MnKat gene: --p-trunc-len-f 188 --p-trunc-len-r 110 --p-max-ee-f 3 --p-max-
168 ee-r 3 [51]. The sequences were further clustered into operational taxonomic units (OTUs)
169 using the VSEARCH algorithm at the following thresholds of sequence similarity: 99% for
170 16S rRNA gene; 96% for AOA *amoA* gene; 96% for AOA MnKat gene. The taxonomy of the
171 OTUs was identified by VSEARCH using the SILVA database (r132) [53] for the 16S rRNA
172 gene and the Alves RJE et al. [54] reference data set for the AOA *amoA* gene. For further
173 analyses, the 16S rRNA and the AOA *amoA* gene OTU tables were rarefied to even depths of
174 49,352 and 42,891 reads, respectively.

175 For phylogenetic analyses, representative full-length sequences of the AOA 16S rRNA,
176 *amoA*, and MnKat genes were obtained from the NCBI database. Alignments of the derived
177 sequences were performed using MAFFT (v7.453) [55]. A maximum likelihood phylogenetic
178 tree was constructed with IQ-TREE (v1.6.12) [56].

179

180 **Catalase activity assays**

Three strains of AOA ("*Ca*. Nitrosocosmicus oleophilus" MY3, *Nitrosoarchaeum koreense* MY1, and *Nitrososphaera viennensis* EN76) and one strain of AOB (*Nitrosomonas europaea* ATCC 19718) were grown under optimal conditions [57]. After oxidizing 1 mM ammonia, the cells were harvested by centrifugation (5,000 × g for 20 min at 25 °C). The harvested cells were washed three times using a basal artificial freshwater medium (AFM) [57], which is devoid of ammonia, trace elements, and pyruvate. Subsequently, 2 ml aliquots of cell suspension were filled into a respiration chamber fitted with contactless oxygen sensor spots (OXSP5, PyroScience, Germany) and maintained for 10–20 min before H_2O_2 injection. The FireSting fiber-optical oxygen meter FSO2-1 (PyroScience, Germany) operation and two-point calibration followed the manufacturer's instructions. The reaction chambers were set at the optimal growth temperature for each strain [57] in a water bath (NB-304, N-BIOTEK, Republic of Korea) and stirred with a magnetic stirrer (MIXdrive 1 XS, 2mag AG, Germany) at 1,000 rpm.

Soil slurry experiment

For soil slurry experiments, the bulk soil composited from five subsamples from the pepper plant experiment was sieved (2-mm-mesh size) to remove plant debris and stones. Aliquots of the fresh bulk soil (0.25 g) were incubated in 25-cm^3 cell culture flasks (SPL Life Sciences, Republic of Korea) containing 10 mL of AFM. The medium contained NH_4Cl (1.5 mM), $NaHCO_3$ (2 mM), and MES buffer (pH 6.5; 3 mM). Allylthiourea (50 μM), an inhibitor of AOB growth [58], was used to focus on the response of soil AOA to H_2O_2 amendment. The cultures were incubated under aerobic conditions in the dark at 30 °C in a static incubator with intermittent mixing. During the experiment, H_2O_2 was amended twice daily to reach final

204 concentrations of 0–30 μM. Nitrite and nitrate were measured using spectrophotometric
205 methods as previously described [57] for the estimation of nitrification activity. For DNA
206 extraction, soil aliquots were obtained from the slurry samples by centrifugation (8,000 × *g* for
207 20 min at 25 °C) and were stored at −80 °C.

208 To estimate the biotic and abiotic decomposition rates of H_2O_2 in soil slurries, H_2O_2
209 concentrations in fresh bulk soils and autoclaved soil slurries were measured using ISO-HPO-
210 100 (WPI, UK) amperometric sensors, with an Apollo 4000 System (WPI, UK). For H_2O_2
211 measurements, soil slurries were stirred using a MS-500 magnetic stirrer (Duksan General
212 Science CO., Republic of Korea) at 1,500 rpm. The electrode was calibrated against freshly
213 prepared H_2O_2 solutions in the range of 0–10 μM in AFM at 25 °C.

214

215 **AOA MnKat gene expression assay**

216 Total RNA was extracted from each 2 g of bulk and rhizosphere soils of the pepper plants using
217 a RNeasy PowerSoil Total RNA Kit (Qiagen, USA) according to the manufacturer's
218 instructions. RNA was eluted in 100 μL of RNase-free water. After removing the DNA from
219 the eluent by treatment with DNase, a SuperScript IV VILO ezDNAse kit (Thermo Fisher
220 Scientific, USA) was used for cDNA synthesis. The concentrations of RNA and cDNA were
221 determined using a Qubit 4 fluorometer (Thermo Fisher Scientific, USA).

222 The relative expression of the AOA MnKat gene in bulk and rhizosphere soils was
223 estimated using a "Ca. Nitrosocosmicus" clade-specific housekeeping gene, *rpoB*, and AOA
224 *amoA* gene (see Table S2). The primer pair for quantifying the *rpoB* gene (nsc-rpoB2884F: 5'-
225 TAYGGWTTYAAGCAYAGTGG-3', nsc-rpoB3320R 5'- TGAGTTTAAATGTSGCWCC -3')

was newly designed using *rpoB* sequences retrieved from "*Ca.* Nitrosocosmicus" clade-genomes (see Fig. S1). The "*Ca.* Nitrosocosmicus" clade-specific *rpoB* gene was amplified via the following steps: 95 °C for 3 min; followed by 40 cycles at 95 °C for 45 s, 59 °C for 45 s, 72 °C for 45 s; and 72 °C for 5 min.

Statistical analysis

All statistical analyses were conducted using the R statistical software (v4.1.2) and R Studio (v2022.02.3). Microbial diversity analysis and data visualization were performed using the R packages phyloseq (v1.26.0) [59], vegan (v2.5-3) [60], and ggplot2 (v3.1.0) [61]. Processed amplicon sequence reads were imported using phyloseq [59]. Non-metric multidimensional scaling (NMDS) analysis and principal coordinate analysis (PCoA) based on Bray-Curtis dissimilarity metrics were used in Vegan [60] to compare the microbial communities between the samples. The ordination analysis patterns were statistically tested using permutational multivariate analysis of variance (PERMANOVA) and analysis of similarity (ANOSIM) with adonis2 and vegdist, respectively, which are part of the vegan packages in R [60]. Indicator species were identified using the indval function of labdsv package (v2.0-1) [62]. Samples from the same compartment were treated as a group for indicator species analysis.

Results

16S rRNA gene amplicon-based archaeal community analysis in pepper and ginseng rhizosphere soils

The prokaryotic communities in bulk and rhizosphere soils of pepper plant were examined using 16S rRNA gene amplicon sequencing during the plant vegetative (60-day-old) and reproductive (90-day-old) growth phases. The compositions and diversities of prokaryotic communities in pepper plant rhizosphere soils differed from those in bulk soils regardless of growth phase (see more details in Supplementary Results and Discussion) (Fig. S2). Archaea were less abundant in rhizosphere soils (0.88 ± 0.20%) compared to bulk soils (4.03 ± 0.48%) in both plant growth phases (Table S4). Members of the phylum *Nitrososphaerota*, which were abundant in both the rhizosphere and bulk soils, accounted for a significant proportion of total archaeal 16S rRNA gene reads (over 93.9%). They were also the eighth most abundant prokaryotic phyla detected, with the majority of their 16S rRNA gene operational taxonomic units (OTUs) (99% similarity cut-off) belonging to three AOA groups (I.1a, I.1a-associated, and I.1b). When compared to other AOM, such as *Nitrosomonadaceae* (the family that includes AOB) and *Nitrospiraceae* (the family that includes both complete ammonia oxidizers [Comammox] and nitrite oxidizers), OTUs belonging to AOA were the most abundant in both bulk and rhizosphere soils of pepper plants (Fig. S3).

Interestingly, distinct AOA communities were observed on the NMDS plot between bulk and rhizosphere soils (Fig. 1A), with a low-stress value (Stress = 0.029), and ANOSIM analysis supported this difference ($R = 0.993$, $P < 0.001$). Furthermore, the difference between plant growth phases had no effect on the AOA communities in the rhizosphere soils (Fig. 1A), as was observed for the total prokaryotic community (Fig. S2B). To identify OTUs that

268 contributed to the discrimination of the AOA communities between bulk and rhizosphere soils,
269 an indicator species analysis was performed at the OTU level. Among the AOA OTUs, only
270 16S_OTU41 was significantly more abundant in the rhizosphere soils (IndVal: 0.66, $q < 0.01$)
271 (Fig. 1B). This OTU is closely related to members of the clade "*Ca*. Nitrosocosmicus" in group
272 I.1b, with > 99.5% 16S rRNA sequence similarity (Fig. 2A). A comparison of the relative
273 abundances of the AOA 16S rRNA gene OTUs showed that 16S_OTU41 was the single most
274 abundant AOA OTU in the rhizosphere soils (averaging 53.6% of the total AOA 16S rRNA
275 gene reads) (Fig. 1B). On the other hand, two AOA OTUs were dominant in the bulk soils
276 (16S_OTU12, accounting for 31.0% of the total AOA 16S rRNA gene reads; 16S_OTU1,
277 accounting for 13.0% of the total AOA 16S rRNA gene reads) (Fig. 1B), and they were closely
278 related to fosmid clone 54d9 of group I.1b and the clade "*Ca.* Nitrosotenuis" of group I.1a,
279 respectively (Fig. 2A).

280 For comparison, prokaryotic communities of perennial ginseng plants (2-, 4-, and 6-
281 year-old) obtained in a different geographical region were analyzed (Table S5). As observed
282 for pepper plants (Fig. S2A and Table S4), AOA were the most dominant archaea in both bulk
283 and rhizosphere soils, and their relative abundance decreased in the rhizosphere soils of the 4-
284 and 6-year-old ginseng plants compared to 2-year-old ginseng plants (Table S5). Accordingly,
285 4- and 6-year-old ginseng plants were used for further analysis. Both rhizosphere prokaryotic
286 and AOA communities of the ginseng plants consistently clustered based on the AOA 16S
287 rRNA gene profiles but were distinct from those of the bulk soils, regardless of the plant age
288 (Stress: 0.060; ANOSIM, $R = 0.933$, $P < 0.001$) (Fig. 1C). Notably, 16S_OTU41 related to "*Ca.*
289 Nitrosocosmicus" was also the most abundant OTU (accounting for 47.52% of total AOA 16S
290 rRNA gene reads) in the rhizosphere of the ginseng plants and predominantly contributed to
291 the clustering of the AOA communities of the rhizosphere soils (IndVal: 0.83, $q < 0.01$) (Figs.

1D and 2A) as observed in the pepper plants. In contrast to the pepper plants, one AOA OTU was dominant in the bulk soils (16S_OTU169, accounting for 72.2% of the total AOA 16S rRNA gene reads, and was closely related to the clade "*Ca.* Nitrosotalea" of group I.1a-associated (Fig. 1D and 2A).

AOA *amoA* gene amplicon-based AOA community analysis

The AOA *amoA* gene amplicon sequencing analysis supported the presence of distinct AOA communities in the rhizosphere *vs.* bulk soils of pepper plants (Stress: 0.038; ANOSIM: R = 0.816, $P < 0.001$) (Fig. 1E). Four "*Ca*. Nitrosocosmicus"-related *amoA* OTUs (amoA_OTU8, -13, -20, and -46), grouped under the *amoA* clade NS-ζ (Zeta) [54] (Fig. 2B), had the highest relative abundance (Fig. 1F) and strongly contributed to the clustering of the AOA communities in rhizosphere soils (IndVal > 0.98). On the other hand, the two most abundant bulk soil-associated AOA *amoA* OTUs, amoA_OTU2 and -16, were affiliated to the *amoA* clades NS-δ (Delta)-1 and NP-η (Eta)-1, respectively (Figs. 1F and 2B). These *amoA* clades correspond to the AOA clades fosmid clone 54d9 and "*Ca.* Nitrosotenuis", respectively (Fig. 2B). The number of *amoA* gene reads was summed for each AOA clade and compared between bulk and rhizosphere soils (Fig. 1G). Consistent with the results on the OTU level, the relative abundance of *amoA* clade NS-ζ AOA, representing the genus "*Ca.* Nitrosocosmicus", was significantly higher in the rhizosphere soils compared to the bulk soils. These *amoA*-based results are highly consistent with the AOA 16S rRNA gene profiles (Figs. 1A and 1B).

The AOA *amoA* gene amplicon sequencing analysis also confirmed the clear segregation of the AOA communities between bulk and rhizosphere soils in the ginseng plants,

as observed in pepper plants (Stress: 0.076; ANOSIM, $R = 0.940$, $P < 0.001$) (Fig. 1H). Furthermore, the relative abundance of the clade NS-ζ significantly increased in the rhizosphere soils, while that of the clade NT-α-1 (i.e., I.1a-associated) decreased, which was consistent with the results of the AOA 16S rRNA gene analysis (Fig. 1I). However, the notable increase in the relative abundance of the clades NS-δ-1 and NP-η-1 in the ginseng rhizosphere soils (Fig. 1I) was unexpected considering the AOA 16S rRNA gene analysis results (Fig. 1D).

Abundance of AOA MnKat gene in rhizosphere soils

Members of the genus "*Ca.* Nitrosocosmicus" possess genomic, morphological, and physiological properties distinct from other AOA [63, 64, 65, 66]. They possess genes that encode a putative MnKat [63, 64, 65, 66] (Fig. 2 and Fig. S4). Despite the presence of MnKat genes in their genomes, catalase activity in these AOA has not yet been directly demonstrated experimentally. Nonetheless, the ability of "*Ca*. Nitrosocosmicus oleophilus" to grow in the absence of H_2O_2 scavengers, unlike other AOA, has already highlighted the presence of an active MnKat [63, 67]. To test for catalase activity, we performed whole-cell assays with different AOM. As expected, the heme-catalase-containing AOB strain (*Nitrosomonas europaea* ATCC 19718) [68], which was used as a positive control, generated O_2 in the presence of H_2O_2 (Fig. 3A). Similarly, O_2 generation in the presence of H_2O_2 was detected for "*Ca*. Nitrosocosmicus oleophilus" MY3 (Fig. 3B), consistent with the proposed activity of its MnKat. In contrast, O_2 generation was not observed in the tested catalase gene-negative AOA, *Nitrosarchaeum koreense* MY1 (clade NP-γ (Gamma)-2.2; group I.1a), and *Nitrososphaera viennensis* EN76 (clade NS-α (Alpha)-3; group I.1b) (Figs. 3C and 3D). Based on these observations, we hypothesized that catalase activity can be one of the important factors

337 associated with the dominance and survival of the "*Ca.* Nitrosocosmicus"-related AOA in the
338 rhizosphere AOA community of pepper and ginseng plants. Coincidently, catalase-containing
339 bacterial OTUs were abundant in the rhizosphere soils of the pepper plants compared to bulk
340 soils (Fig. S5 and Dataset S1). Specifically, 96.9% of the top 63 rhizosphere-associated OTUs
341 (indicated by a positive value in log_2fold) are known to have catalase gene or activity. In
342 contrast, only 11.3% of the top 79 bulk-associated OTUs (indicated by a negative value in
343 log_2fold) have a catalase gene or activity (Fig. S5 and Dataset S1).

344 Thus, by using qPCR, we quantified the relative abundance of MnKat-containing AOA
345 in the rhizosphere soils of pepper and ginseng plants by comparing the copy numbers of the
346 AOA MnKat genes relative to the *amoA* genes. Based on the newly designed PCR primer pair
347 targeting AOA MnKat genes, we found that all amplified MnKat gene sequences belonged to
348 AOA, and more importantly, sequences associated with "*Ca*. Nitrosocosmicus"-related AOA
349 were predominant in the rhizosphere and bulk soils (Table S6 and Dataset S2). In addition,
350 AOA *amoA* gene copy numbers per gram of soil were lower in rhizosphere soils compared to
351 bulk soils of the pepper plants (Fig. 4A). On the other hand, AOA MnKat gene copy numbers
352 in 60- and 90-day-old rhizosphere soils were comparable to those in bulk soils (Fig. 4A).
353 Overall, the copy number ratios of AOA MnKat genes to *amoA* genes were significantly higher
354 in pepper plant rhizosphere soils than in bulk soils (Fig. 4B). The qPCR and sequencing
355 analysis results of MnKat-containing AOA in ginseng plants (Figs. 4C, 4D, Table S6) were
356 consistent with those of pepper plants (Figs. 4A, 4B, Table S6). Overall results from both plants
357 revealed that: 1) Most of the amplified MnKat gene sequences are associated with "*Ca.*
358 Nitrosocosmicus" and, 2) The copy number ratios AOA MnKat genes to *amoA* genes were
359 higher in the rhizosphere soils than in bulk soils.

Enrichment of MnKat-containing AOA from soil by H_2O_2 treatment

To investigate the selective enrichment of MnKat-containing AOA in H_2O_2-amended soils, bulk soil slurries from the pepper plant experiment were incubated with 1.5 mM ammonium chloride in the presence of 0–30 µM H_2O_2 (Fig. S6). Because H_2O_2 is rapidly decomposed by soil microorganisms and abiotic processes (Fig. S7), resulting in a short half-life (14.9 min at 10 µM H_2O_2), it was added to the soil slurries twice daily during the incubation period. Ammonia oxidation was gradually inhibited as the concentration of amended H_2O_2 in the soil slurry increased (Fig. S6). The copy number ratios of AOA MnKat genes to *amoA* genes increased in proportion to the concentration of H_2O_2 amended (Fig. S8), indicating that the presence of H_2O_2 in the soil selectively enriched catalase-containing AOA.

AOA community analysis of the soil slurries amended with H_2O_2 was performed using amplicon sequencing of prokaryotic 16S rRNA and AOA *amoA* genes (Fig. S9). We found a clear segregation between the slurry samples with different H_2O_2 concentrations based on the AOA 16S rRNA gene profiles (Stress: 0.020; ANOSIM, $R = 0.825$, $P < 0.001$). A cluster of the soil slurries with 30 µM H_2O_2 was especially distinct from the others (Fig. S9A). The relative abundances of 16S_OTU41 belonging to the clade "*Ca*. Nitrosocosmicus" increased proportionally to the H_2O_2 concentration based on the AOA 16S rRNA gene amplicon sequencing results (Figs. 2A and S9B). In contrast, the relative abundance of other AOA 16S rRNA gene OTUs (16S_OTU1, -2, and -89), belonging to the clades *Nitrosarchaeum* and "*Ca*. Nitrosotenuis" of group I.1a, significantly decreased as the concentration of H_2O_2 increased (Figs. 2A and S9B). Lastly, the relative abundance of 16S_OTU12, affiliated with the clade fosmid clone 54d9, remained unchanged across all H_2O_2 concentrations (Figs. 2A and S9B).

383 The segregation of AOA communities in the soil slurry samples based on H_2O_2
384 concentrations added was also supported by AOA *amoA* gene amplicon sequencing data (Stress:
385 0.049; ANOSIM, $R = 0.673$, $P < 0.001$) (Fig. S9C). The soil slurry sample cluster with 30 µM
386 H_2O_2 was especially distinct from the others (Fig. S9C); this finding was also consistent with
387 the AOA 16S rRNA gene-based analysis (Fig. S9A). Furthermore, the relative abundances of
388 *amoA* clades NS-δ-1, NS-δ-2, NS-ζ, and NS-α-3 increased as H_2O_2 concentrations increased
389 (Fig. S9D). Also, both the AOA 16S rRNA and *amoA* gene profiles revealed a significant
390 increase in the relative abundance of "*Ca.* Nitrosocosmicus"-related AOA (clade NS-ζ) (Figs.
391 2A, S9B, S9D). Surprisingly, as the H_2O_2 concentrations increased, so did the relative
392 abundance of clade NS-δ-1 *amoA* genes (related to the *amoA* gene on the fosmid clone 54d9),
393 contrary to what was observed in the AOA 16S rRNA gene profiles analysis (Figs. 2A, S9B).
394 However, the relative abundance of other AOA clades in group I.1a (*amoA* clades NP-η-1 and
395 NP-γ-2.2) decreased with increasing H_2O_2 concentrations (Fig. S9D), as observed in the AOA
396 16S rRNA gene profiles analysis (Figs. 2A, S9B). Taken together, these results support the
397 hypothesis that resistance to H_2O_2 is important in the selection of MnKat-containing AOA in
398 soil habitats with elevated H_2O_2 concentrations, such as the plant rhizosphere.

399

400 **Expression of AOA MnKat gene in rhizosphere soils**

401 To demonstrate AOA MnKat gene expression in rhizosphere soils, transcripts of AOA MnKat
402 genes were quantified using cDNA generated from mRNA extracted from pepper plant
403 rhizosphere soils and bulk soils. In addition, a "*Ca.* Nitrosocosmicus" clade-specific
404 housekeeping gene, *rpoB*, and AOA *amoA* gene were quantified to estimate the relative
405 abundance of AOA MnKat gene transcripts in rhizosphere soils. The metatranscriptomics data

406 revealed that the relative abundance of AOA MnKat gene transcripts to AOA *amoA* and "*Ca*.
407 Nitrosocosmicus" clade *rpoB* gene transcripts in rhizosphere soils was not significantly
408 different from those in bulk soils (Fig. S10), indicating possible constitutive expression of AOA
409 MnKat genes in soils.

410

411 **Discussion**

412 There have been extensive studies on rhizosphere microbial communities, as the rhizosphere
413 microbiome affects the survival of plants under stress conditions such as those caused by
414 climate change, pathogen infection, etc. [1, 2, 3]. Despite their potential importance in plant
415 growth and development, archaea are only rarely included in rhizosphere microbiomes [31, 69].
416 AOA are especially abundant in terrestrial environments and play a key role in the soil nitrogen
417 cycle, necessitating additional research into their interactions with plant roots [36, 69]. Patterns
418 of prokaryotic communities formed in the analyzed rhizosphere soils (see more details in
419 Supplementary Results and Discussion) (Fig. S2 and Tables S4 and S5) distinct from the bulk
420 soils of pepper plants were consistent with previous studies on other plant species [4, 8, 9, 70].
421 Distinct AOA communities in rhizosphere soils of pepper and ginseng plants relative to bulk
422 soils were revealed by 16S rRNA and *amoA* genes amplicon sequencing profiles (Figs. 1A, 1C,
423 1E, and 1H), indicating a niche differentiation of AOA between bulk and rhizosphere soils of
424 the plants.

425 Overall, we observed a decrease in the relative abundance of AOA in rhizosphere soils
426 of pepper and ginseng plants compared to bulk soils (Fig. S2A and Tables S4 and S5), which
427 contradicts previous findings [31, 71, 72, 73, 74, 75, 76]. Also, despite having a low relative

abundance in pepper plant rhizosphere soils, AOA still outnumbered other ammonia-oxidizing microorganisms (Fig. S3). Consequently, their low abundance may decrease nitrification activity near plant roots, which is desirable to reduce N losses and increase N fertilizer use efficiency [72, 77]. This finding might explain why gross nitrification rates in rhizosphere soils were lower than in bulk soils, despite higher gross N mineralization rates [78]. In particular, AOA related to "*Ca*. Nitrosocosmicus" were notably the most abundant in the rhizosphere soil s based on 16S rRNA and *amoA* gene amplicon analyses (Figs. 1B, 1D, 1F, 1G, 1I, and 2). Interestingly, among genome-sequenced AOA, MnKat genes are exclusively present in members of the genus "*Ca.* Nitrosocosmicus" and of the species "*Ca.* Nitrososphaera evergladensis" [63, 64, 65, 79] (Fig. 2). Phylogenetic analysis of MnKat genes (Fig. S4) revealed that *Nitrososphaerota* MnKat genes were closely related to those found in the bacterial phylum *Terrabacteria*, which includes common soil bacteria such as *Actinomycetota* and *Bacillota* [66]. In addition, these genes differed from those found in closely related archaeal phyla, *Ca.* Thermoproteota and *Ca.* Methanobacteriota, implying that horizontal gene transfer events between archaea and bacteria shaped the evolutionary history of MnKat gene (Fig. S4).

Catalase activity was measured in "*Ca.* Nitrosocosmicus oleophilus" MY3 (Fig. 3B), a strain closely related to AOA that was enriched in pepper and ginseng rhizospheres (Fig. 2). The AOA MnKat, whose active site is predicted to be stable under low H_2O_2 levels compared with the heme catalase [80], may provide an evolutionary advantage at low H_2O_2 levels (< 3 μM), which can completely inhibit the nitrification activity of catalase-negative AOA [81, 82]. Based on the documented selection of MnKat-encoding AOA in rhizospheres of pepper and ginseng plants, as well as the experimental confirmation of catalase activity in a related AOA isolate, it is tempting to speculate that resistance to H_2O_2 is one of the important factors shaping AOA communities in rhizospheres. Consistently, we observed that the copy number ratios of

AOA MnKat gene to *amoA* gene were significantly higher in rhizosphere soils of pepper and ginseng plants than bulk soils (Figs. 4B, 4D). The dominance of AOA MnKat gene sequences closely related to "*Ca.* Nitrosocosmicus" in rhizosphere soils (Table S6) corroborated the results of AOA 16S rRNA and *amoA* gene analyses (Fig. 1).

Soil characteristics [4, 5, 7, 8, 9] and host phylogeny [4, 13, 14] are considered to be important determinants of rhizosphere microbial community composition and function. Even plant genotype-specific microbial communities have been observed in the rhizosphere of some plant species [5, 7]. Despite the different life cycles, phylogeny, and geographic locations of the pepper and ginseng plants studied here, distinct AOA communities in the rhizosphere soils relative to the bulk soils were observed, which was also attributable to the predominance of the MnKat-containing members of "*Ca.* Nitrosocosmicus" (Figs. 1B, 1D, 1F, 1G, 1I and 2). In this context, it is important to note that the dominant phylotype, C1b.A1 (representing the clones TRC23-30 and TRC23-38), belonging to *Nitrososphaerota* (formerly known as Crenarchaeota), was found to predominantly colonize the roots of tomato (*Solanum lycopersicum* L. in the order Solanales) grown in soil from a Wisconsin field [83]. This phylotype is closely related to "*Ca.* Nitrosocosmicus oleophilus" MY3 with 99.7% 16S rRNA gene sequence similarity, suggesting that closely related members of "*Ca.* Nitrosocosmicus" are selectively enriched in various agriculturally important plants and that the enrichment of the AOA in the plant rhizosphere may be widespread, regardless of geographical location and plant phylogeny.

In addition to the *amoA* clade NS-ζ containing members of the genus "*Ca.* Nitrosocosmicus", the AOA *amoA* gene reads of the clade NS-δ-1 harboring the fosmid clone 54D9 *amoA* sequence were also abundant in the H_2O_2-amended soil slurries (Fig. S9D) and the rhizosphere soils of ginseng plants (Fig. 1I), but not in the pepper plants (Fig. 1G). It is yet

475 unknown whether clade NS-δ-1 members have MnKat genes. The prominent increases in the
476 relative abundance of the AOA *amoA* gene reads from clade 54D9 (Figs. 1I and S9D) are in
477 stark contrast with the findings from the analysis of AOA 16S rRNA gene amplicon reads (Figs.
478 1D, 2A and S9B). Thus, we cannot rule out the possibility that the PCR primer set used to
479 construct the AOA *amoA* gene amplicon libraries is biased towards clade NS-δ-1 *amoA* genes.

480 Oxygen supply is crucial for plant roots, not only for cell respiration but also for the
481 formation of reactive oxygen species, including H_2O_2. H_2O_2 is a ubiquitous metabolic by-
482 product of aerobic unicellular and multicellular organisms [84, 85, 86, 87] that plays an
483 important role in developmental and physiological processes in plant roots. H_2O_2 is involved
484 in loosening cell walls for cell elongation in roots via peroxidase-mediated lignin
485 formation [43, 88] and accumulates in the differentiation zone and the cell wall of root hairs
486 during the formation of fine roots in *Arabidopsis* (*Arabidopsis thaliana* in order
487 Brassicales) [44]. It was observed that H_2O_2 production increased in a specific region of fine
488 roots after K^+ deprivation [89]. Similarly, H_2O_2 release from seedlings roots into the
489 environment has been observed [44, 90, 91, 92]. Furthermore, mycorrhizae mediated an
490 increase in H_2O_2 release from the roots of trifoliate orange to alleviate drought stress [93].
491 Recently, it was proposed that the rhizosphere is a widespread but previously unappreciated
492 hotspot for ROS production, with hydroxyl radicals, which represent ROS species, periodically
493 accumulating up to > 2 μM in rice plant rhizosphere soil pore water after six hour of light
494 exposure [94]. Thus, plant roots trigger the release of H_2O_2 into their surroundings and
495 thereby chemically shape the rhizosphere habitat. In addition to plant roots, soil
496 microorganisms are known to release ROS [46, 47].

497 In the soil slurry experiments, we demonstrated that H_2O_2 amendment in bulk soils

498 increased the abundance of MnKat-containing AOA in a concentration-dependent manner (Fig.
499 S8). In addition, AOA from the clade "*Ca*. Nitrosocosmicus" became dominant in H_2O_2-
500 amended soil slurries (Fig. S9B), and the copy number ratios of AOA MnKat genes to *amoA*
501 genes increased as the concentration of H_2O_2 increased (Fig. S8B). The toxic effects of H_2O_2
502 on AOA were previously assessed with group I.1a, where ammonia oxidation was completely
503 inhibited at levels of 0.2–3.0 μM H_2O_2 [81, 82]. Consistently, the nitrification activity and
504 abundance of AOA decreased in H_2O_2-amended soil slurries (Figs. S6 and S7). This might
505 explain the decrease in gross nitrification rates in the rhizosphere [78]. Further, "*Ca*.
506 Nitrosocosmicus" MnKat genes were found to be constitutively expressed in pepper plant
507 rhizosphere soils and bulk soils (Fig. S10). Taken together, our results imply that rhizosphere
508 H_2O_2 may be an important factor in the selection of MnKat-containing AOA in the plant
509 rhizosphere. Interestingly, metagenomic and metatranscriptomic analyses of the rhizosphere
510 microbial communities of cucumber (*Cucumis sativus* L. in the order Cucurbitales) and wheat
511 (*Triticum aestivum* L. in the order Poales) plants identified the enrichment and expression of
512 prokaryotic catalase genes, which were suggested to be associated with root colonization [95].
513 The dominance of catalase-containing bacterial OTUs in rhizosphere soils of pepper plants
514 over bulk soils (Fig. S5 and Dataset S1) observed in this study corresponds to these findings.
515 It is plausible that H_2O_2 levels in rhizosphere environments may be inhibitory to catalase-
516 negative microbes such as group I.1a and I.1a-associated AOA. In suspended aquatic
517 environments, the growth of catalase-negative AOA could be supported by coexisting catalase-
518 positive microbes [82, 96, 97]. Hence, further study will be needed to reveal if such an
519 interaction exists between catalase-positive microbes and catalase-negative AOA in soil
520 environments. Therefore, we propose that the catalase activity of microorganisms in
521 rhizospheres may serve as a microbial stress response. It may also modulate developmental

522 and physiological processes in plant roots, as well redox dynamics and biogeochemical
523 processes in soil.

524 Despite the presence of MnKat gene in "*Ca.* Nitrososphaera evergladensis" genome,
525 OTUs related to this AOA were not dominant in the analyzed microbial community in
526 rhizosphere soils (Table S6). Thus, while catalase activity is a very plausible explanation for
527 the selection of members of the genus "*Ca.* Nitrosocosmicus" in the rhizosphere, it should be
528 noted that the genomes of these ammonia-oxidizers also encode various distinct traits that may
529 individually or collectively confer higher rhizosphere fitness compared to other AOA. For
530 example, tolerance to high salinity [64] and acidic pH [98] as well as the ability for biofilm
531 formation [63] observed in "*Ca.* Nitrosocosmicus" members may support survival in the
532 rhizosphere and/or help establish interactions with plant roots. Further, the higher concentration
533 of ammonia in rhizosphere soils compared to bulk soils [99] might facilitate the competitive
534 success of members of "*Ca.* Nitrosocosmicus", which possess a lower affinity and lower
535 specific affinity for ammonia than other AOA [100] in the rhizosphere. Thus, more research is
536 needed to determine how catalase activity contributes to the enrichment of "*Ca.*
537 Nitrosocosmicus" members in the rhizospheres of various plants.

538 The nitrification process, which converts ammonia to nitrite and then to nitrate,
539 strongly affects the availability of nitrogen species for plant roots [101]. The available
540 inorganic nitrogen species ratio (ammonium:nitrate) is significant to plant growth by
541 influencing cellular pH maintenance and energy efficiency of nitrogen assimilation in
542 plants [102, 103]. Due to their abundance, AOA, especially catalase-containing "*Ca.*
543 Nitrosocosmicus" members, as demonstrated in this study, are considered to be key players
544 mediating the nitrification process in the rhizosphere [72]. Song et al. demonstrated that "*Ca.*

Nitrosocosmicus oleophilus" MY3 cells colonized the root surface of *Arabidopsis* plants, and proposed that volatile compounds emitted by "*Ca*. Nitrosocosmicus oleophilus" MY3 could elicit induced systemic resistance [104]. Taken together, the selection of catalase-containing AOA of the genus "*Ca.* Nitrosocosmicus" in the rhizosphere of several agriculturally important plants hints at a previously overlooked AOA-plant interaction. Our understanding of AOA-plant interactions in the rhizosphere is still in its infancy, and this study highlights a key clade of AOA with already available cultured representatives for further mechanistic analyses in this important research field.

Acknowledgments

This work was supported by the Basic Science Research Program through the National Research Foundation of Korea (NRF) funded by the Korean government (Ministry of Education) (2020R1A6A1A06046235), the NRF grants funded by the Korean government (Ministry of Science and ICT) (2021R1A2C3004015), and the National Institute of Agricultural Science, Ministry of Rural Development Administration, Republic of Korea (PJ01700703). J-HG was supported by the NRF grant funded by the MSIT (RS-2023-00213601). M-YJ was supported by the NRF grant funded by MSIT (NRF-2021R1C1C1008303 and NRF-2022R1A4A503144711).

Ethics declarations

Ethics approval and consent to participate

566 Not applicable.

567

568 **Consent for publication**

569 Not applicable.

570

571 **Competing interests**

572 The authors declare no competing interests.

573

574 **Availability of data and materials**

575 The 16S rRNA, AOA *amoA* and AOA MnKat genes amplicon sequencing data generated in
576 this study have been deposited in NCBI under the BioProject ID: PRJNA905906.

577

578

References

1. Lemanceau, P, Barret, M, Mazurier, S, Mondy, S, Pivato, B, Fort, T, *et al.* Chapter Five - Plant communication with associated microbiota in the spermosphere, rhizosphere and phyllosphere. In: Becard G, editor. Advances in Botanical Research. 1st ed: Academic Press; 2017. p. 101-133.

2. Korenblum, E, Dong, Y, Szymanski, J, Panda, S, Jozwiak, A, Massalha, H, *et al.* Rhizosphere microbiome mediates systemic root metabolite exudation by root-to-root signaling. Proc Natl Acad Sci USA. 2020; 117:3874-3883.

3. Pascale, A, Proietti, S, Pantelides, IS, Stringlis, IA. Modulation of the root microbiome by plant molecules: the basis for targeted disease suppression and plant growth promotion. Front Plant Sci. 2020; 10:1741.

4. Bulgarelli, D, Rott, M, Schlaeppi, K, Ver Loren van Themaat, E, Ahmadinejad, N, Assenza, F, *et al.* Revealing structure and assembly cues for *Arabidopsis* root-inhabiting bacterial microbiota. Nature. 2012; 488:91-95.

5. Lundberg, DS, Lebeis, SL, Paredes, SH, Yourstone, S, Gehring, J, Malfatti, S, *et al.* Defining the core *Arabidopsis thaliana* root microbiome. Nature. 2012; 488:86-90.

6. Peiffer Jason, A, Spor, A, Koren, O, Jin, Z, Tringe Susannah, G, Dangl Jeffery, L, *et al.* Diversity and heritability of the maize rhizosphere microbiome under field conditions. Proc Natl Acad Sci U S A. 2013; 110:6548-6553.

7. Bulgarelli, D, Garrido-Oter, R, Münch, PC, Weiman, A, Dröge, J, Pan, Y, *et al.* Structure and function of the bacterial root microbiota in wild and domesticated barley. Cell Host Microbe. 2015; 17:392-403.

8. Edwards, J, Johnson, C, Santos-Medellín, C, Lurie, E, Podishetty, NK, Bhatnagar, S, *et al.* Structure, variation, and assembly of the root-associated microbiomes of rice. Proc Natl Acad Sci USA. 2015; 112:E911-E920.

9. Schreiter, S, Ding, G-C, Heuer, H, Neumann, G, Sandmann, M, Grosch, R, *et al.* Effect of the soil type on the microbiome in the rhizosphere of field-grown lettuce. Front Microbiol. 2014; 5:144.

10. Paterson, E, Gebbing, T, Abel, C, Sim, A, Telfer, G. Rhizodeposition shapes rhizosphere microbial community structure in organic soil. New Phytol. 2007; 173:600-610.

11. Marschner, H, Römheld, V, Horst, WJ, Martin, P. Root-induced changes in the rhizosphere: Importance for the mineral nutrition of plants. Zeitschrift für Pflanzenernahrung und Bodenkunde. 1986; 149:441-456.

12. Dennis, PG, Miller, AJ, Hirsch, PR. Are root exudates more important than other sources of rhizodeposits in structuring rhizosphere bacterial communities? FEMS Microbiol Ecol. 2010; 72:313-327.

13. Haichar, F, el Z, Marol, C, Berge, O, Rangel-Castro, JI, Prosser, JI, Balesdent, J, *et al.* Plant host habitat and root exudates shape soil bacterial community structure. ISME J. 2008; 2:1221-1230.

14. Müller, H, Berg, C, Landa, BB, Auerbach, A, Moissl-Eichinger, C, Berg, G. Plant genotype-specific archaeal and bacterial endophytes but similar *Bacillus* antagonists colonize Mediterranean olive trees. Front Microbiol. 2015; 6:138.

15. Berendsen, RL, Pieterse, CMJ, Bakker, PAHM. The rhizosphere microbiome and plant health. Trends Plant Sci. 2012; 17:478-486.

16. Hu, L, Robert, CAM, Cadot, S, Zhang, X, Ye, M, Li, B, *et al.* Root exudate metabolites drive plant-soil feedbacks on growth and defense by shaping the rhizosphere microbiota. Nat Commun. 2018; 9:2738.

17. DeAngelis, KM, Brodie, EL, DeSantis, TZ, Andersen, GL, Lindow, SE, Firestone, MK. Selective progressive response of soil microbial community to wild oat roots. ISME J. 2009; 3:168-178.

18. Vranova, V, Rejsek, K, Skene, KR, Janous, D, Formanek, P. Methods of collection of plant root exudates in relation to plant metabolism and purpose: A review. J Plant Nutr Soil Sci. 2013; 176:175-199.

19. Pausch, J, Kuzyakov, Y. Carbon input by roots into the soil: quantification of rhizodeposition from root to ecosystem scale. Glob Chang Biol. 2018; 24:1-12.

20. Pausch, J, Tian, J, Riederer, M, Kuzyakov, Y. Estimation of rhizodeposition at field scale: upscaling of a ^{14}C labeling study. Plant Soil. 2013; 364:273-285.

21. Olanrewaju, OS, Ayangbenro, AS, Glick, BR, Babalola, OO. Plant health: feedback effect of root exudates-rhizobiome interactions. Applied microbiology and biotechnology. 2019; 103:1155-1166.

22. Reinhold-Hurek, B, Bünger, W, Burbano, CS, Sabale, M, Hurek, T. Roots shaping their microbiome: global hotspots for microbial activity. Annu Rev Phytopathol. 2015; 53:403-424.

23. Sasse, J, Martinoia, E, Northen, T. Feed your friends: do plant exudates shape the root microbiome? Trends Plant Sci. 2018; 23:25-41.

24. Pieterse, CMJ, Van der Does, D, Zamioudis, C, Leon-Reyes, A, Van Wees, SCM.

646 Hormonal modulation of plant immunity. Annu Rev Cell Dev Biol ANNU REV CELL
647 DEV BI. 2012; 28:489-521.

648 25. Piasecka, A, Jedrzejczak-Rey, N, Bednarek, P. Secondary metabolites in plant innate
649 immunity: conserved function of divergent chemicals. New Phytol. 2015; 206:948-964.

650 26. Bamji, SF, Corbitt, C. Glyceollins: Soybean phytoalexins that exhibit a wide range of
651 health-promoting effects. J Funct Foods. 2017; 34:98-105.

652 27. Sarr, PS, Ando, Y, Nakamura, S, Deshpande, S, Subbarao, GV. Sorgoleone release
653 from sorghum roots shapes the composition of nitrifying populations, total bacteria, and
654 archaea and determines the level of nitrification. Biol Fertil Soils. 2020; 56:145-166.

655 28. Preston, GM. Profiling the extended phenotype of plant pathogens. Mol Plant Pathol.
656 2017; 18:443-456.

657 29. Hayat, S, Faraz, A, Faizan, M. Root exudates: composition and impact on plant–
658 microbe interaction. In: Iqbal A, Husain FM, editors. Biofilms in Plant and Soil Health.
659 1st ed: Wiley Blackwell; 2017. p. 179-193.

660 30. Karlsson, AE, Johansson, T, Bengtson, P. Archaeal abundance in relation to root and
661 fungal exudation rates. FEMS Microbiol Ecol. 2012; 80:305-311.

662 31. Taffner, J, Bergna, A, Cernava, T, Berg, G. Tomato-associated archaea show a cultivar-
663 specific rhizosphere effect but an unspecific transmission by seeds. Phytobiomes J.
664 2020; 4:133-141.

665 32. Chelius, MK, Triplett, EW. The diversity of archaea and bacteria in association with
666 the roots of *Zea mays* L. Microb Ecol. 2001; 41:252-263.

667 33. Sliwinski, MK, Goodman, RM. Comparison of crenarchaeal consortia inhabiting the

668 rhizosphere of diverse terrestrial plants with those in bulk soil in native environments.
669 Appl Environ Microbiol. 2004; 70:1821-1826.

670 34. Wang, H, Bier, R, Zgleszewski, L, Peipoch, M, Omondi, E, Mukherjee, A, *et al.*
671 Distinct distribution of archaea from soil to freshwater to estuary: implications of
672 archaeal composition and function in different environments. Front Microbiol. 2020;
673 11:576661.

674 35. Liu, N, Hu, H, Ma, W, Deng, Y, Liu, Y, Hao, B, *et al.* Contrasting biogeographic
675 patterns of bacterial and archaeal diversity in the top- and subsoils of temperate
676 grasslands. mSystems. 2019; 4:e00566-00519.

677 36. Leininger, S, Urich, T, Schloter, M, Schwark, L, Qi, J, Nicol, GW, *et al.* Archaea
678 predominate among ammonia-oxidizing prokaryotes in soils. Nature. 2006; 442:806-
679 809.

680 37. Wang, J-T, Cao, P, Hu, H-W, Li, J, Han, L-L, Zhang, L-M, *et al.* Altitudinal distribution
681 patterns of soil bacterial and archaeal communities along Mt. Shegyla on the Tibetan
682 Plateau. Microb Ecol. 2015; 69:135-145.

683 38. Mamet, SD, Lamb, EG, Piper, CL, Winsley, T, Siciliano, SD. Archaea and bacteria
684 mediate the effects of native species root loss on fungi during plant invasion. ISME J.
685 2017; 11:1261-1275.

686 39. Oren, A, Garrity, GM. Valid publication of the names of forty-two phyla of prokaryotes.
687 Int J Syst Evol Microbiol. 2021; 71:005056.

688 40. DeLong, EF. Everything in moderation: archaea as 'non-extremophiles'. Curr Opin
689 Genet Dev. 1998; 8:649-654.

690 41. Neill, SJ, Desikan, R, Hancock, JT. Nitric oxide signalling in plants. New Phytol. 2003;
691 159:11-35.

692 42. Coskun, D, Britto, DT, Shi, W, Kronzucker, HJ. Nitrogen transformations in modern
693 agriculture and the role of biological nitrification inhibition. Nat Plants. 2017; 3:17074.

694 43. Passardi, F, Penel, C, Dunand, C. Performing the paradoxical: how plant peroxidases
695 modify the cell wall. Trends Plant Sci. 2004; 9:534-540.

696 44. Dunand, C, Crèvecoeur, M, Penel, C. Distribution of superoxide and hydrogen peroxide
697 in *Arabidopsis* root and their influence on root development: possible interaction with
698 peroxidases. New Phytol. 2007; 174:332-341.

699 45. Becana, M, Aparicio-Tejo, P, Irigoyen, JJ, Sanchez-Diaz, M. Some enzymes of
700 hydrogen-peroxide metabolism in leaves and root-nodules of *Medicago sativa*. Plant
701 Physiol. 1986; 82:1169-1171.

702 46. Ikuta, S, Matuura, K, Imamura, S, Misaki, H, Horiuti, Y. Oxidative Pathway of Choline
703 to Betaine in the Soluble Fraction Prepared from Arthrobacter globiformis. J Biochem.
704 1977; 82:157-163.

705 47. Kontchou, CY, Blondeau, R. Isolation and characterization of hydrogen peroxide
706 producing Aerococcus sp. from soil samples. FEMS Microbiol Lett. 1990; 68:323-327.

707 48. Awala, SI, Gwak, J-H, Kim, Y-M, Kim, S-J, Strazzulli, A, Dunfield, PF, *et al.*
708 Verrucomicrobial methanotrophs grow on diverse C3 compounds and use a homolog
709 of particulate methane monooxygenase to oxidize acetone. ISME J. 2021; 15:3636-
710 3647.

711 49. Nolan, T, Hands, RE, Ogunkolade, W, Bustin, SA. SPUD: A quantitative PCR assay

712 for the detection of inhibitors in nucleic acid preparations. Anal Biochem. 2006;
713 351:308-310.

714 50. Martin, M. Cutadapt removes adapter sequences from high-throughput sequencing
715 reads. EMBnet j. 2011; 17:10-12.

716 51. Callahan, BJ, McMurdie, PJ, Rosen, MJ, Han, AW, Johnson, AJA, Holmes, SP.
717 DADA2: High-resolution sample inference from Illumina amplicon data. Nat Methods.
718 2016; 13:581-583.

719 52. Rognes, T, Flouri, T, Nichols, B, Quince, C, Mahé, F. VSEARCH: a versatile open
720 source tool for metagenomics. PeerJ. 2016; 4:e2584.

721 53. Quast, C, Pruesse, E, Yilmaz, P, Gerken, J, Schweer, T, Yarza, P, *et al.* The SILVA
722 ribosomal RNA gene database project: improved data processing and web-based tools.
723 Nucleic Acids Res. 2013; 41:D590-D596.

724 54. Alves, RJE, Minh, BQ, Urich, T, von Haeseler, A, Schleper, C. Unifying the global
725 phylogeny and environmental distribution of ammonia-oxidising archaea based on
726 *amoA* genes. Nat Commun. 2018; 9:1517.

727 55. Katoh, K, Standley, DM. MAFFT multiple sequence alignment software version 7:
728 improvements in performance and usability. Mol Biol Evol. 2013; 30:772-780.

729 56. Nguyen, L-T, Schmidt, HA, von Haeseler, A, Minh, BQ. IQ-TREE: a fast and effective
730 stochastic algorithm for estimating maximum-likelihood phylogenies. Mol Biol Evol.
731 2015; 32:268-274.

732 57. Gwak, J-H, Jung, M-Y, Hong, H, Kim, J-G, Quan, Z-X, Reinfelder, JR, *et al.* Archaeal
733 nitrification is constrained by copper complexation with organic matter in municipal

734 wastewater treatment plants. ISME J. 2020; 14:335-346.

735 58. Shen, T, Stieglmeier, M, Dai, J, Urich, T, Schleper, C. Responses of the terrestrial
736 ammonia-oxidizing archaeon Ca. Nitrososphaera viennensis and the ammonia-
737 oxidizing bacterium Nitrosospira multiformis to nitrification inhibitors. FEMS
738 Microbiol Lett. 2013; 344:121-129.

739 59. McMurdie, PJ, Holmes, S. Phyloseq: an R package for reproducible interactive analysis
740 and graphics of microbiome census data. PLoS One. 2013; 8:e61217.

741 60. Oksanen, J, Blanchet, FG, Kindt, R, Legendre, P, Minchin, P, O'hara, R, *et al.* Vegan:
742 Community ecology package. R package version 2.5-32018.

743 61. Wickham, H. ggplot2: elegant graphics for data analysis. New York: Springer; 2016.

744 62. Roberts, DW. labdsv: ordination and multivariate analysis for ecology. R package
745 version 2.0-1;. 2017.

746 63. Jung, M-Y, Kim, J-G, Sinninghe Damsté, JS, Rijpstra, WIC, Madsen, EL, Kim, S-J, *et*
747 *al.* A hydrophobic ammonia-oxidizing archaeon of the *Nitrosocosmicus* clade isolated
748 from coal tar-contaminated sediment. Environ Microbiol Rep. 2016; 8:983-992.

749 64. Liu, L, Liu, M, Jiang, Y, Lin, W, Luo, J. Production and excretion of polyamines to
750 tolerate high ammonia, a case study on soil ammonia-oxidizing archaeon "*Candidatus*
751 Nitrosocosmicus agrestis". mSystems. 2021; 6:e01003-01020.

752 65. Sauder, LA, Albertsen, M, Engel, K, Schwarz, J, Nielsen, PH, Wagner, M, *et al.*
753 Cultivation and characterization of *Candidatus* Nitrosocosmicus exaquare, an
754 ammonia-oxidizing archaeon from a municipal wastewater treatment system. ISME J.
755 2017; 11:1142-1157.

66. Abby, SS, Kerou, M, Schleper, C. Ancestral reconstructions decipher major adaptations of ammonia-oxidizing archaea upon radiation into moderate terrestrial and marine environments. MBio. 2020; 11:e02371-02320.

67. Lehtovirta-Morley, LE, Ross, J, Hink, L, Weber, EB, Gubry-Rangin, C, Thion, C, *et al.* Isolation of '*Candidatus* Nitrosocosmicus franklandus', a novel ureolytic soil archaeal ammonia oxidiser with tolerance to high ammonia concentration. FEMS Microbiol Ecol. 2016; 92:fiw057.

68. Wood, NJ, Sørensen, J. Catalase and superoxide dismutase activity in ammonia-oxidising bacteria. FEMS Microbiol Ecol. 2001; 38:53-58.

69. Moissl-Eichinger, C, Pausan, M, Taffner, J, Berg, G, Bang, C, Schmitz, RA. Archaea are interactive components of complex microbiomes. Trends Microbiol. 2018; 26:70-85.

70. Yeoh, YK, Paungfoo-Lonhienne, C, Dennis, PG, Robinson, N, Ragan, MA, Schmidt, S, *et al.* The core root microbiome of sugarcanes cultivated under varying nitrogen fertilizer application. Environ Microbiol. 2016; 18:1338-1351.

71. Chen, X-P, Zhu, Y-G, Xia, Y, Shen, J-P, He, J-Z. Ammonia-oxidizing archaea: important players in paddy rhizosphere soil? Environ Microbiol. 2008; 10:1978-1987.

72. Thion, CE, Poirel, JD, Cornulier, T, De Vries, FT, Bardgett, RD, Prosser, JI. Plant nitrogen-use strategy as a driver of rhizosphere archaeal and bacterial ammonia oxidiser abundance. FEMS Microbiol Ecol. 2016; 92:fiw091.

73. Wattenburger, CJ, Gutknecht, J, Zhang, Q, Brutnell, T, Hofmockel, K, Halverson, L. The rhizosphere and cropping system, but not arbuscular mycorrhizae, affect ammonia oxidizing archaea and bacteria abundances in two agricultural soils. Agric, Ecosyst

779 Environ, Appl Soil Ecol. 2020; 151:103540.

780 74. Simon, HM, Dodsworth, JA, Goodman, RM. Crenarchaeota colonize terrestrial plant
781 roots. Environ Microbiol. 2000; 2:495-505.

782 75. Ai, C, Liang, G, Sun, J, Wang, X, He, P, Zhou, W. Different roles of rhizosphere effect
783 and long-term fertilization in the activity and community structure of ammonia
784 oxidizers in a calcareous fluvo-aquic soil. Soil Biol Biochem. 2013; 57:30-42.

785 76. Herrmann, M, Saunders Aaron, M, Schramm, A. Archaea dominate the ammonia-
786 oxidizing community in the rhizosphere of the freshwater macrophyte *Littorella*
787 *uniflora*. Appl Environ Microbiol. 2008; 74:3279-3283.

788 77. Norton, J, Ouyang, Y. Controls and adaptive management of nitrification in agricultural
789 soils. Front Microbiol. 2019; 10:1931.

790 78. Herman, DJ, Johnson, KK, Jaeger, CH, Schwartz, E, Firestone, MK. Root influence on
791 nitrogen mineralization and nitrification in *Avena barbata* rhizosphere soil. Soil Sci Soc
792 Am J. 2006; 70:1504-1511.

793 79. Zhalnina, KV, Dias, R, Leonard, MT, Dorr de Quadros, P, Camargo, FAO, Drew, JC,
794 *et al.* Genome sequence of *Candidatus* Nitrososphaera evergladensis from group I.1b
795 enriched from everglades soil reveals novel genomic features of the ammonia-oxidizing
796 archaea. PLoS One. 2014; 9:e101648.

797 80. Whittaker, JW. Non-heme manganese catalase—the 'other' catalase. Arch Biochem
798 Biophys. 2012; 525:111-120.

799 81. Bayer, B, Pelikan, C, Bittner, MJ, Reinthaler, T, Könneke, M, Herndl, GJ, *et al.*
800 Proteomic response of three marine ammonia-oxidizing archaea to hydrogen peroxide

and their metabolic interactions with a heterotrophic alphaproteobacterium. mSystems. 2019; 4:e00181-00119.

82. Kim, J-G, Park, S-J, Sinninghe Damsté, JS, Schouten, S, Rijpstra, WIC, Jung, M-Y, *et al.* Hydrogen peroxide detoxification is a key mechanism for growth of ammonia-oxidizing archaea. Proc Natl Acad Sci USA. 2016; 113:7888-7893.

83. Simon, HM, Jahn, CE, Bergerud, LT, Sliwinski, MK, Weimer, PJ, Willis, DK, *et al.* Cultivation of mesophilic soil crenarchaeotes in enrichment cultures from plant roots. Appl Environ Microbiol. 2005; 71:4751-4760.

84. Veal, EA, Day, AM, Morgan, BA. Hydrogen peroxide sensing and signaling. Mol Cell. 2007; 26:1-14.

85. Zamocky, M, Furtmuller, PG, Obinger, C. Evolution of catalases from bacteria to humans. Antioxid Redox Signal. 2008; 10:1527-1548.

86. Stone, JR, Yang, S. Hydrogen peroxide: a signaling messenger. Antioxid Redox Signal. 2006; 8:243-270.

87. Imlay, JA. Cellular defenses against superoxide and hydrogen peroxide. Annu Rev Biochem. 2008; 77:755-776.

88. Tobimatsu, Y, Schuetz, M. Lignin polymerization: how do plants manage the chemistry so well? Curr Opin Biotechnol. 2019; 56:75-81.

89. Shin, R, Schachtman, DP. Hydrogen peroxide mediates plant root cell response to nutrient deprivation. Proc Natl Acad Sci USA. 2004; 101:8827-8832.

90. Lee, SH, Singh, AP, Chung, GC. Rapid accumulation of hydrogen peroxide in cucumber roots due to exposure to low temperature appears to mediate decreases in

water transport. J Exp Bot. 2004; 55:1733-1741.

91. Zhao, Y, Zhang, Y, Liu, F, Wang, R, Huang, L, Shen, W. Hydrogen peroxide is involved in methane-induced tomato lateral root formation. Plant Cell Rep. 2019; 38:377-389.

92. Liszkay, A, van der Zalm, E, Schopfer, P. Production of reactive oxygen intermediates ($O_2^{\cdot-}$, H_2O_2, and $^{\cdot}OH$) by maize roots and their role in wall loosening and elongation growth. Plant Physiol. 2004; 136:3114-3123.

93. Huang, Y-M, Zou, Y-N, Wu, Q-S. Alleviation of drought stress by mycorrhizas is related to increased root H_2O_2 efflux in trifoliate orange. Sci Rep. 2017; 7:42335.

94. Dai, H, Wu, B, Chen, B, Ma, B, Chu, C. Diel Fluctuation of Extracellular Reactive Oxygen Species Production in the Rhizosphere of Rice. Environ Sci Technol ENVIRON SCI TECHNOL. 2022; 56:9075-9082.

95. Ofek-Lalzar, M, Sela, N, Goldman-Voronov, M, Green, SJ, Hadar, Y, Minz, D. Niche and host-associated functional signatures of the root surface microbiome. Nat Commun. 2014; 5:4950.

96. Jung, M-Y, Park, S-J, Kim, S-J, Kim, J-G, Sinninghe Damsté Jaap, S, Jeon Che, O, *et al.* A Mesophilic, Autotrophic, Ammonia-Oxidizing Archaeon of Thaumarchaeal Group I.1a Cultivated from a Deep Oligotrophic Soil Horizon. Appl Environ Microbiol. 2014; 80:3645-3655.

97. Jung, M-Y, Park, S-J, Min, D, Kim, J-S, Rijpstra, WIC, Sinninghe Damsté Jaap, S, *et al.* Enrichment and Characterization of an Autotrophic Ammonia-Oxidizing Archaeon of Mesophilic Crenarchaeal Group I.1a from an Agricultural Soil. Appl Environ Microbiol. 2011; 77:8635-8647.

98. Jung, M-Y, Gwak, J-H, Rohe, L, Giesemann, A, Kim, J-G, Well, R, *et al.* Indications for enzymatic denitrification to N2O at low pH in an ammonia-oxidizing archaeon. ISME J. 2019; 13:2633-2638.

99. Koranda, M, Schnecker, J, Kaiser, C, Fuchslueger, L, Kitzler, B, Stange, CF, *et al.* Microbial processes and community composition in the rhizosphere of European beech – the influence of plant C exudates. Soil Biol Biochem. 2011; 43:551-558.

100. Jung, M-Y, Sedlacek, CJ, Kits, KD, Mueller, AJ, Rhee, S-K, Hink, L, *et al.* Ammonia-oxidizing archaea possess a wide range of cellular ammonia affinities. ISME J. 2022; 16:272-283.

101. Beeckman, F, Motte, H, Beeckman, T. Nitrification in agricultural soils: impact, actors and mitigation. Curr Opin Biotechnol. 2018; 50:166-173.

102. Neumann, G, Römheld, V. Rhizosphere chemistry in relation to plant nutrition. In: Marschner P, editor. Marschner's mineral nutrition of higher plants. Rhizosphere Chemistry in Relation to Plant Nutrition. 3rd ed: Academic Press; 2012. p. 347-368.

103. Xu, G, Fan, X, Miller, AJ. Plant nitrogen assimilation and use efficiency. Annu Rev Plant Biol. 2012; 63:153-182.

104. Song, GC, Im, H, Jung, J, Lee, S, Jung, M-Y, Rhee, S-K, *et al.* Plant growth-promoting archaea trigger induced systemic resistance in *Arabidopsis thaliana* against *Pectobacterium carotovorum* and *Pseudomonas syringae*. Environ Microbiol. 2019; 21:940-948.

105. Kalyaanamoorthy, S, Minh, BQ, Wong, TKF, von Haeseler, A, Jermiin, LS. ModelFinder: fast model selection for accurate phylogenetic estimates. Nat Methods. 2017; 14:587-589.

869 **Figure legends**

870 **Fig. 1: Distinct AOA communities in bulk and rhizosphere soils of pepper and ginseng**
871 **plants.**

872 **A, C** Non-metric multidimensional scaling (NMDS) plot using Bray–Curtis dissimilarity
873 metrics of AOA communities in bulk and rhizosphere soils, based on AOA 16S rRNA gene
874 profiles of pepper plants ($n = 25$) (**A**) and ginseng plants ($n = 29$) (**C**). **B, D** Relative abundances
875 (% of the total 16S rRNA gene reads) of AOA 16S rRNA gene OTUs (> 0.04% of the mean of
876 relative abundances) of pepper plants (**B**) and ginseng plants (**D**). Results of indicator species
877 analysis are shown above each OTU's bar with the IndVal value in parenthesis. Indicator values
878 (IndVal > 0.6, q < 0.01) are displayed for rhizosphere (R) or bulk soil (B). **E, H** NMDS plot
879 using Bray–Curtis dissimilarity metrics of AOA communities in bulk and rhizosphere soils,
880 based on AOA *amoA* gene profiles of pepper plants ($n = 20$) (**E**) and ginseng plants ($n = 29$)
881 (**H**). **F** Relative abundances (% of the total AOA *amoA* gene reads) of AOA *amoA* gene OTUs
882 (> 1% of the mean of relative abundances) of pepper plants. Results of indicator species
883 analysis are shown above each OTU's bar with the IndVal value in parenthesis. Indicator values
884 (IndVal > 0.6, q < 0.01) are displayed for rhizosphere (R) or bulk soil (B). **G, I** Relative
885 abundance (% of each AOA clade relative abundances as the sum of AOA *amoA* OTU
886 abundances) of AOA clade (> 3% of the mean of relative abundances) of pepper plants (**G**) and
887 ginseng plants (**I**). Statistical significance was determined using Student's *t*-tests (**$P < 0.005$,
888 ***$P < 0.0005$).

889

Fig. 2: Maximum likelihood phylogenetic trees of AOA 16S rRNA and *amoA* genes.

A Phylogenetic tree of AOA 16S rRNA gene sequences reconstructed using IQ-TREE. The GTR+F+I+G4 model was determined using ModelFinder Plus [105] within IQ-TREE [56]. **B** Phylogenetic tree of AOA *amoA* genes reconstructed using IQ-TREE. The TIM2+F+R5 model was determined using ModelFinder Plus [105] within IQ-TREE [56]. Branch supports for 1,000 replicates were obtained using the ultrafast bootstrap and SH-aLRT tests. Branch supports ≥ 95% are indicated by black circles. MnKat gene-containing AOA are depicted in bold and blue letters. A truncated MnKat gene-containing AOA is shown in bold and brown letters. Each AOA group is indicated by different colored backgrounds (group I.1a, blue; group I.1a-associated, yellow; group I.1b, red; and thermophilic AOA, gray).

Fig. 3: Catalase activity of AOB and AOA strains.

An assessment of oxygen production in the presence of 30 μM H_2O_2 in an AOB strain (**A)** and three AOA strains (**B**–**D)**. The results of two biological replicates are shown.

Fig. 4: Abundance of AOA *amoA* and MnKat genes.

A Copy numbers of AOA *amoA* and MnKat genes in each soil compartment at two different growth phases of the pepper plants (60- and 90-day-old). **B** The copy number ratios (%) of AOA MnKat gene to *amoA* gene calculated from (**A**) are shown. Error bars represent the

909 standard deviations of five replicates. **C** The copy numbers of AOA *amoA* and MnKat genes at
910 three different ages (2-, 4-, and 6-year-old) and in each compartment (bulk and rhizosphere
911 soils). **D** The copy number ratios (%) of AOA MnKat gene to *amoA* gene calculated from (**C**)
912 are shown. R represents rhizosphere soil; B represents bulk soil. Error bars represent standard
913 deviations of biological replicates (B, three replicates; R, five replicates). Statistical
914 significance was determined using Student's *t*-tests (*$P < 0.05$, **$P < 0.005$, ***$P < 0.0005$).

915

Fig 1

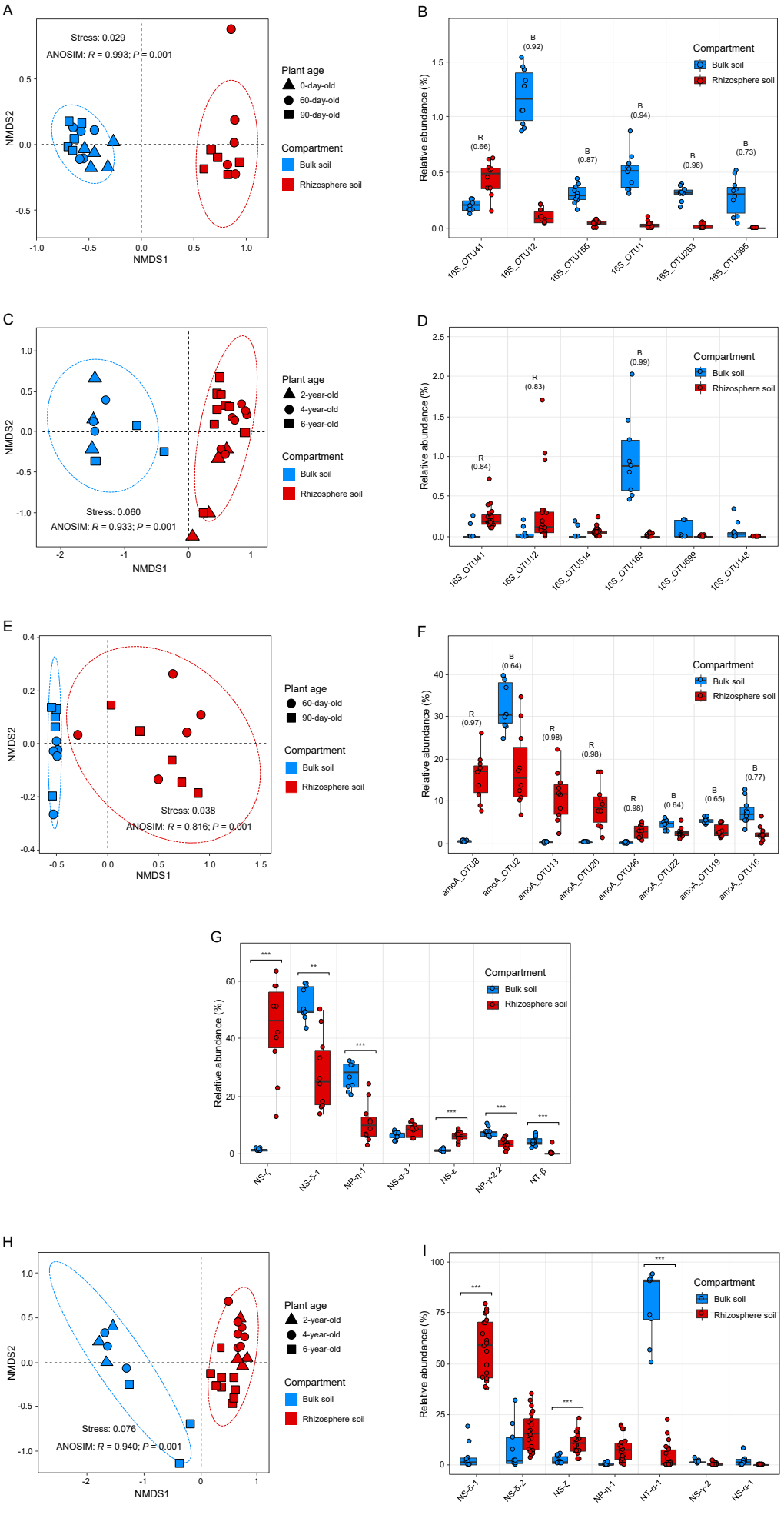

Fig. 2

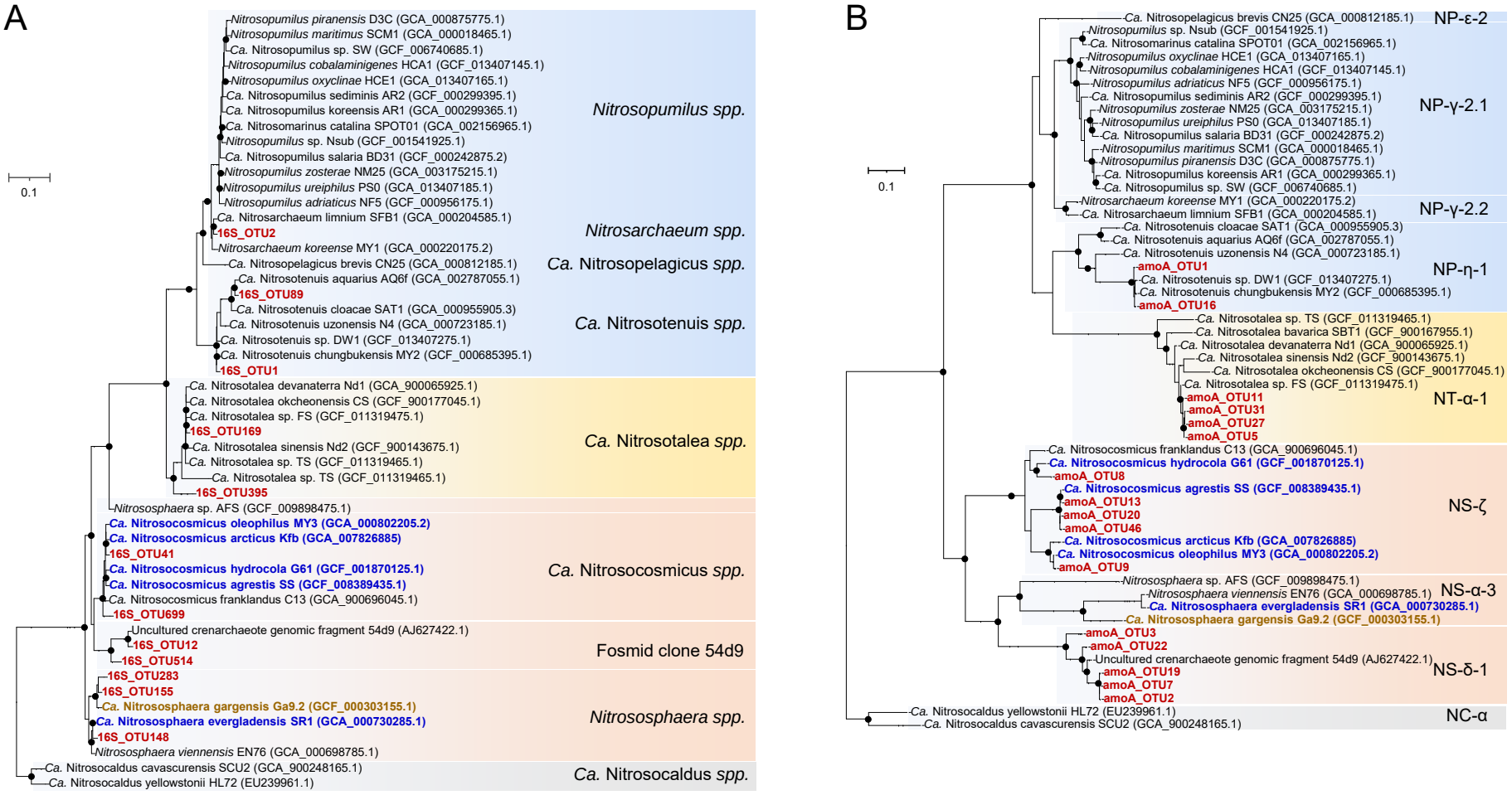

Fig. 3

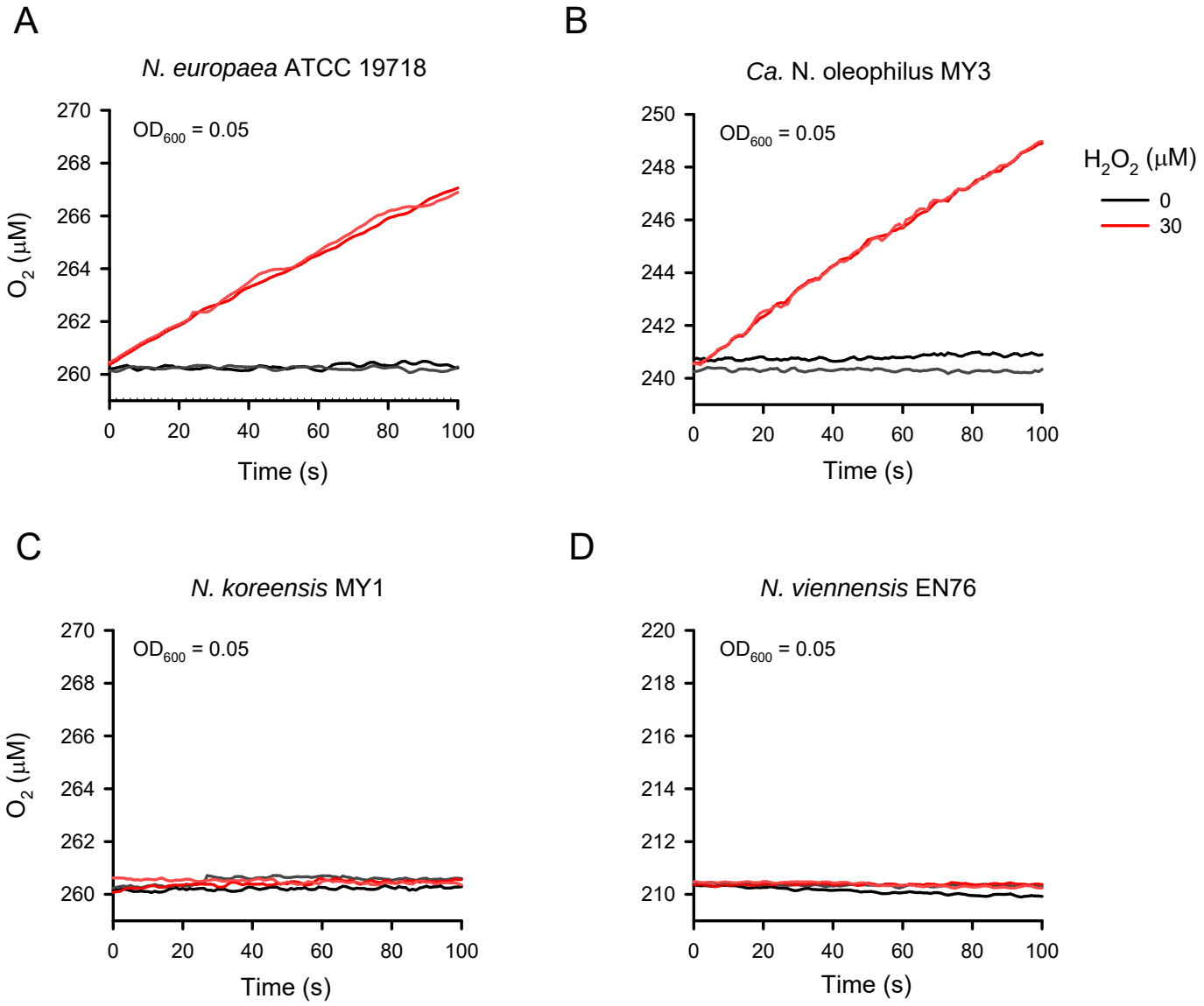

Fig. 4